Hindawi Publishing Corporation
International Journal of Electrochemistry
Volume 2012, Article ID 323560, 9 pages
doi:10.1155/2012/323560

Research Article

High Tap Density Spherical $Li[Ni_{0.5}Mn_{0.3}Co_{0.2}]O_2$ Cathode Material Synthesized via Continuous Hydroxide Coprecipitation Method for Advanced Lithium-Ion Batteries

Shunyi Yang, Xianyou Wang, Xiukang Yang, Ziling Liu, Qiliang Wei, and Hongbo Shu

Key Laboratory of Environmentally Friendly Chemistry and Applications of Ministry of Education, School of Chemistry, Xiangtan University, Hunan, Xiangtan 411105, China

Correspondence should be addressed to Xianyou Wang, xywang@xtu.edu.cn

Received 30 September 2011; Accepted 14 December 2011

Academic Editor: Valentin Mirceski

Spherical $[Ni_{0.5}Mn_{0.3}Co_{0.2}](OH)_2$ precursor with narrow size distribution and high tap density has been successfully synthesized by a continuous hydroxide coprecipitation, and $Li[Ni_{0.5}Mn_{0.3}Co_{0.2}]O_2$ is then prepared by mixing the precursor with 6% excess Li_2CO_3 followed by calcinations. The tap density of the obtained $Li[Ni_{0.5}Mn_{0.3}Co_{0.2}]O_2$ powder is as high as 2.61 g cm^{-3}. The powders are characterized by X-ray diffraction (XRD), X-ray photoelectron spectroscopy (XPS), scanning electron microscope (SEM), particle size distribution (PSD), and charge/discharge cycling. The XRD studies show that the prepared $Li[Ni_{0.5}Mn_{0.3}Co_{0.2}]O_2$ has a well-ordered layered structure without any impurity phases. Good packing properties of spherical secondary particles (about 12 μm) consisted of a large number of tiny-thin plate-shape primary particles (less than 1 μm), which can be identified from the SEM observations. In the voltage range of 3.0–4.3 V and 2.5–4.6 V, $Li[Ni_{0.5}Mn_{0.3}Co_{0.2}]O_2$ delivers the initial discharge capacity of approximately 175 and 214 mAh g^{-1} at a current density of 32 mA g^{-1}, and the capacity retention after 50 cycles reaches 98.8% and 90.2%, respectively. Besides, it displays good high-temperature characteristics and excellent rate capability.

1. Introduction

During the past decade, lithium ion batteries have been extensively investigated and widely used; they are not only required to enable the moderately charge/discharge rates applications like mobile phone and portable computer but also to meet an increasing need for new applications such as electric vehicles, which need power sources with both high energy and high power density. Layered $LiNi_{0.5}Mn_{0.5}O_2$ is of great interest as a promising cathode material for lithium secondary batteries because of its higher theoretical capacity (280 mAh g^{-1}) and better structural stability [1–5]. However, some problems, such as uneasy preparation of stoichiometric phases [6], low tapping density [7], and poor rate capability [8], have to be overcome before it is massively applied in the lithium ion battery industry.

Recently, the effects of cobalt doping on the structure and electrochemical behavior of $LiNi_{0.5}Mn_{0.5}O_2$ had been reported by Li et al. [9], and the results showed that cobalt doping for $LiNi_{0.5}Mn_{0.5}O_2$ can easily form stoichiometric $Li[Ni_{0.5}Mn_{0.5-x}Co_x]O_2$ compounds, which possess good electronic conductivity, and thus owning good rate capability. In the series of $LiNi_{0.5}Mn_{0.5-x}Co_xO_2$, $Li[Ni_{0.5}Mn_{0.3}Co_{0.2}]O_2$ can be considered as one of the most promising cathode materials for the application of lithium ion battery, because this composition compromises between the increase of the discharge capacity due to the Co^{3+} and the increase of the thermal stability due to the Mn^{4+} ions. Nevertheless, the characteristics of the $Li[Ni_{0.5}Mn_{0.3}Co_{0.2}]O_2$ strongly depend on the preparation route. Liu et al. [10] stated that the $Li[Ni_{0.5}Mn_{0.3}Co_{0.2}]O_2$ prepared by traditionally mixed hydroxide method in flowing O_2 showed homogeneous phase structure; the lattice parameters of the powder were a = 2.908 Å, c = 14.250 Å, and ratio of I_{003}/I_{104} that represents the degree of cation mixing was 1.50. It delivered the initial discharge capacity of 150 mAh g^{-1} at a current density of 0.2 mA cm^{-2} between 2.75 and 4.2 V, but it showed a poor cycling behavior. Li et al. [11] have reported that

$Li[Ni_{0.5}Mn_{0.3}Co_{0.2}]O_2$ synthesized by solid state reaction in O_2 had an agglomerated morphology; the lattice parameters of the powder were $a \approx 2.87$ Å, $c \approx 14.26$ Å, with ratio of $I_{003}/I_{104} = 1.20$. It exhibited the initial discharge capacity of 172 mAh g^{-1}, and the capacity retention after 25 cycles was less than 85% at a current density of 40 mA g^{-1} (0.4 mA cm^{-2}) between 3.0 and 4.6 V. Above researches [10, 11] had proved that traditionally mixed hydroxide method and solid state reaction method were unsuitable for preparation of $Li[Ni_{0.5}Mn_{0.3}Co_{0.2}]O_2$ with high electrochemical performance and high tap density.

To obtain an ideal $Li[Ni_{0.5}Mn_{0.3}Co_{0.2}]O_2$ cathode material with high discharge capacity, excellent cycling performance and high volume energy density, the morphology and tap density of the material have to be controlled precisely during the preparation process. In general, high tap density particles could be obtained by increasing crystallinity and grain size of crystals, but this will lead to loss of specific discharge capacity. Another way to increase tap density of the material without loss of discharge capacity is to fabricate firstly the precursor of uniform-sized spherical particles by coprecipitation, then to obtain high performance $Li[Ni_{0.5}Mn_{0.3}Co_{0.2}]O_2$. In this paper, a continuous hydroxide coprecipitation method has been developed to prepare a spherical $Li[Ni_{0.5}Mn_{0.3}Co_{0.2}]O_2$ in a self-designed device. During the preparation process, two continuous stirred-tank reactors (CSTR) with same structure are used to control availability the morphology of the precursor. The one is used for coprecipitation reaction, and another is used for ageing process, which will prolong an average residence time of reaction particle in the vessel to get regular and round spherical precursor. The structural properties, morphologies, particle size distributions of the precursor $[Ni_{0.5}Mn_{0.3}Co_{0.2}](OH)_2$, and final product $Li[Ni_{0.5}Mn_{0.3}Co_{0.2}]O_2$ were discussed, and the electrochemical characteristics of the $Li[Ni_{0.5}Mn_{0.3}Co_{0.2}]O_2$ were also investigated in detail.

2. Experimental

2.1. Preparation of $[Ni_{0.5}Mn_{0.3}Co_{0.2}](OH)_2$ Precursor. Spherical $[Ni_{0.5}Mn_{0.3}Co_{0.2}](OH)_2$ was synthesized by a continuous hydroxide coprecipitation under N_2 atmosphere. The details of the coprecipitation apparatus are shown in Figure 1. Initially, the CSTR-1 was filled with distilled water corresponding to 20 vol.% of the reactor, and the pH was then adjusted to 11.0 with proper amount of 3.6 M NH_4OH and 3.6 M NaOH to get an initial solution. The solution was stirred at 800 rpm, and the temperature of the solution was maintained at 50°C by circulating hot water through the jacket of the reactor. The 1.8 M aqueous solution of $NiSO_4 \cdot 6H_2O$, $MnSO_4 \cdot H_2O$, and $CoSO_4 \cdot 7H_2O$ corresponding to a molar composition of Ni : Mn : Co = 5 : 3 : 2 was introduced continuously into the CSTR-1 by a peristaltic pump. At the same time, a 3.6 M aqueous solution of NaOH and desired amount of complexant 3.6 M NH_4OH were separately fed into the reactor. The total feed flow rate was adjusted to assure an average residence time of 10 h in CSTR-1. The liquid product that overflowed out from the CSTR-1 was feed into CSTR-2 for ageing step, which was kept at the same reaction conditions as CSTR-1. Finally, the products that collected continuously from the base of CSTR-2 were filtered, washed, and dried at 110°C for 12 h to obtain $[Ni_{0.5}Mn_{0.3}Co_{0.2}](OH)_2$ precursor.

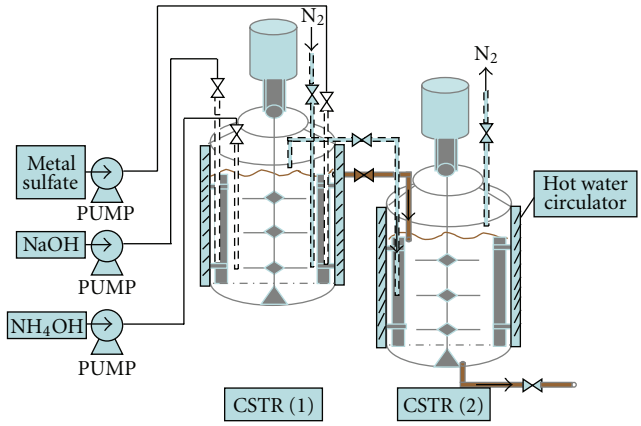

Figure 1: Schematic of device for preparing $[Ni_{0.5}Mn_{0.3}Co_{0.2}](OH)_2$ precursor by continuous coprecipitation.

2.2. Preparation of $Li[Ni_{0.5}Mn_{0.3}Co_{0.2}]O_2$. The $[Ni_{0.5}Mn_{0.3}Co_{0.2}](OH)_2$ precursor was mixed thoroughly with 6% excess of a stoichiometric amount of Li_2CO_3 (molar ratio of 1 : 1.06) to compensate the Li loss on the calcining process. The mixture was preheated at 500°C for 5 h and then calcined at 820°C for 12 h in air to obtain the final product $Li[Ni_{0.5}Mn_{0.3}Co_{0.2}]O_2$.

2.3. Characterization. The chemical composition of the resulting powder was analyzed by atomic absorption spectroscopy (Vario 6 Analytik Jena AG, Jena, Germany). The tap densities of $[Ni_{0.5}Mn_{0.3}Co_{0.2}](OH)_2$ and $Li[Ni_{0.5}Mn_{0.3}Co_{0.2}]O_2$ were determined by Powder Integrative Characteristic Tester (BT-1000, Bettersize Instruments Ltd, China), the vibration amplitude is 3 mm, the vibration frequency is 250 time min^{-1}, and the repeatability precision is less than 1%. The particle size and particle size distribution were measured by Mastersizer-2000 (Malvern Instruments Ltd, England). The phase identification of the sample was performed with a diffractometer (D/Max-3C, Rigaku, Japan) using Cu Kα radiation ($\lambda = 1.54178$ Å) and a graphite monochromator at 36 kV, 20 mA. The scanning rate was 8° min^{-1}, and the scanning range of diffraction angle (2θ) was $10^\circ \leq 2\theta \leq 80^\circ$. X-ray photoelectron spectroscopy (XPS, PHI-5800) measurements were conducted to determine the sample. Al Kα (1486 eV) radiation was the primary excitation source, and the energy scale was adjusted based on the carbon peak in the C1s spectra at 284.6 eV. The morphology of the samples were observed using scanning electron microscopy (JSM-5600LV, JEOL, Japan).

The electrochemical tests of $Li[Ni_{0.5}Mn_{0.3}Co_{0.2}]O_2$ were carried out using coin cells assembled in an argon-filled glove box. In all cells, the cathode was consisted of a mixture of active material (80 wt.%), acetylene black (10 wt.%), graphite (5 wt.%), and polyvinylidene fluoride (5 wt.%) as

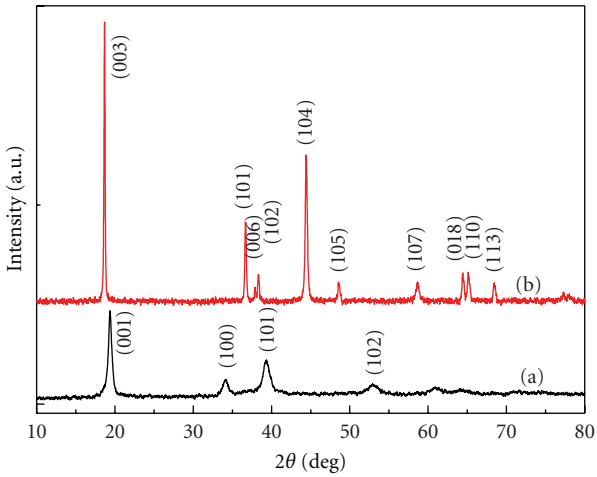

FIGURE 2: XRD patterns of (a) $[Ni_{0.5}Mn_{0.3}Co_{0.2}](OH)_2$ precursor and (b) final product $Li[Ni_{0.5}Mn_{0.3}Co_{0.2}]O_2$.

a binder agent, lithium was served as counter and reference electrodes, a Celgard 2400 was used as separator, and the electrolyte was a 1 M $LiPF_6$ solution in ethylene carbonate (EC)-dimethyl carbonate (DMC) (1 : 1 in volume). Charge/discharge measurements were carried out in Neware battery test system (BTS-XWJ-6.44S-00052, Newell, China).

3. Results and Discussion

Figure 2(a) displays the XRD pattern of the $[Ni_{0.5}Mn_{0.3}Co_{0.2}](OH)_2$ precursor. It can be observed that the XRD pattern of the $[Ni_{0.5}Mn_{0.3}Co_{0.2}](OH)_2$ is almost consistent with the typical fingerprint of $Ni(OH)_2$ structure [12]. All diffraction lines are indexed to a hexagonal structure with a space group of $p\bar{3}m1$. The absence of impurity phases indicates that Ni, Co, and Mn would be homogeneously distributed within $[Ni_{0.5}Mn_{0.3}Co_{0.2}](OH)_2$ particle. The chemical composition of the $[Ni_{0.5}Mn_{0.3}Co_{0.2}](OH)_2$ precursor was analyzed by atomic absorption spectroscopy. The results identify that the element ratio of Ni : Mn : Co is 0.501 : 0.297 : 0.202, the element ratio of Ni : Mn : Co is nearly close to the design value of 5 : 3 : 2. Figure 2(b) illustrates the XRD pattern of the final product $Li[Ni_{0.5}Mn_{0.3}Co_{0.2}]O_2$. It reveals that the as-synthesized powder has the typical structure of a hexagonal α-$NaFeO_2$ type with a space group of $R\bar{3}m$ (no. 166). The diffraction peaks are quite narrow, indicating high crystallinity, and no impurity diffraction peak is observed. The splits in the (006)/(102) and (108)/(110) doublets indicate the formation of a highly ordered α-$NaFeO_2$-type layered structure [13]. Lattice parameters, c/a value, I_{003}/I_{104} value of the $Li[Ni_{0.5}Mn_{0.3}Co_{0.2}]O_2$ are tabulated in Table 1. The calculated lattice parameters of the powder are $a = 2.870$ Å, $c = 14.256$ Å, and $V = 101.690$ Å^3. These data are similar to those observed by other researchers listed in Table 1. The value of $c/a = 4.967$ reveals that the layered structure is formed. In the layered structure, Li^+, transition metal ions and oxygen ion are situated in Figures 3(a), 3(b), and 6(c), respectively. Since the ionic radii of Li^+ (0.76 Å) and Ni^{2+} (0.69 Å) ions are similar, a partial disordering in Figures 3(a) and 3(b) is expected, and it is called "cation mixing" [14, 15]. It has been known that the cation mixing will deteriorate the electrochemical performance of the layered oxide materials. The integrated intensity ratio of I_{003}/I_{104} (R) is sensitive to the cation mixing and usually taken as a measure of the amount of the cation mixing in the series of $LiNiO_2$ families [16, 17]. Higher value of R is desirable for lower amount of the cation mixing. $R < 1.2$ is an indication of undesirable cation mixing [18]. It can be seen from Table 1 that the value of $R = 1.779$ for the as-prepared $Li[Ni_{0.5}Mn_{0.3}Co_{0.2}]O_2$, which indicates the low amount of cation mixing in its layered structure.

TABLE 1: Calculated structure parameters for Li $[Ni_{0.5}Mn_{0.3}Co_{0.2}]O_2$.

Sample	a-axis (Å)	c-axis (Å)	Unit volume (Å^3)	c/a	I_{003}/I_{104}
Prepared $Li[Ni_{0.5}Mn_{0.3}Co_{0.2}]O_2$	2.870	14.256	101.690	4.967	1.779
$Li[Ni_{0.5}Mn_{0.3}Co_{0.2}]O_2$ [10]	2.908	14.250	104.4	4.90	1.50
$Li[Ni_{0.5}Mn_{0.3}Co_{0.2}]O_2$ [11]	~2.87	~14.26	~102	~4.963	1.20

$Li[Ni_{0.5}Mn_{0.3}Co_{0.2}]O_2$ compound was characterized by XPS in order to analyze the chemical composition of the spheres. The XPS emission spectra of $Li[Ni_{0.5}Mn_{0.3}Co_{0.2}]O_2$ and corresponding magnified Mn $2p_{3/2}$, Co $2p_{3/2}$ and Ni $2p_{3/2}$ are presented in Figure 3. In the spectrum of analysis of whole elements as shown in Figure 3(a), the peaks for Li, Mn, Co, Ni, and O originated from $Li[Ni_{0.5}Mn_{0.3}Co_{0.2}]O_2$ are observed. Besides, the peak for C can also be found in the spectrum, which probably came from CO_2 that attached to the surface of the sample. As illustrated in Figure 3(b), the binding energy of Mn $2p_{3/2}$ electron in the $Li[Ni_{0.5}Mn_{0.3}Co_{0.2}]O_2$ is 641.7 eV, which is the same as that of the Li_2MnO_3. These results suggest that the valence of Mn is tetravalent, well consistent with those reported [19]. It can be seen from Figure 3(c) that the Co $2p_{3/2}$ has a characteristic peak with a binding energy of 779.6 eV and can be indexed to the Co^{3+} (the published binding energy of a trivalent Co $2p_{3/2}$ electron is 779.3–779.9 eV [20]). As shown in Figure 3(d), the Ni $2p_{3/2}$ peak is observed at 855.2 eV. Because the standard binding energies of Ni^{2+} and Ni^{3+} are 853.8 and 857.3 eV [21], respectively, it is expected that the valence number of Ni in $Li[Ni_{0.5}Mn_{0.3}Co_{0.2}]O_2$ is a mixture of 2+ and 3+. It is well known that the existence of mixed-valence cations (Ni^{2+}/Ni^{3+}) significantly contributes to the inherent electronic conductivity of electrodes during charge and discharge [22]. Therefore, good electrochemical performance would be expected for the as-prepared $Li[Ni_{0.5}Mn_{0.3}Co_{0.2}]O_2$.

Scanning electron micrographs of the $[Ni_{0.5}Mn_{0.3}Co_{0.2}](OH)_2$ precursor with different magnifications are presented in Figure 4. The secondary particle of precursor has an average size of about 12 μm with homogeneous spherical

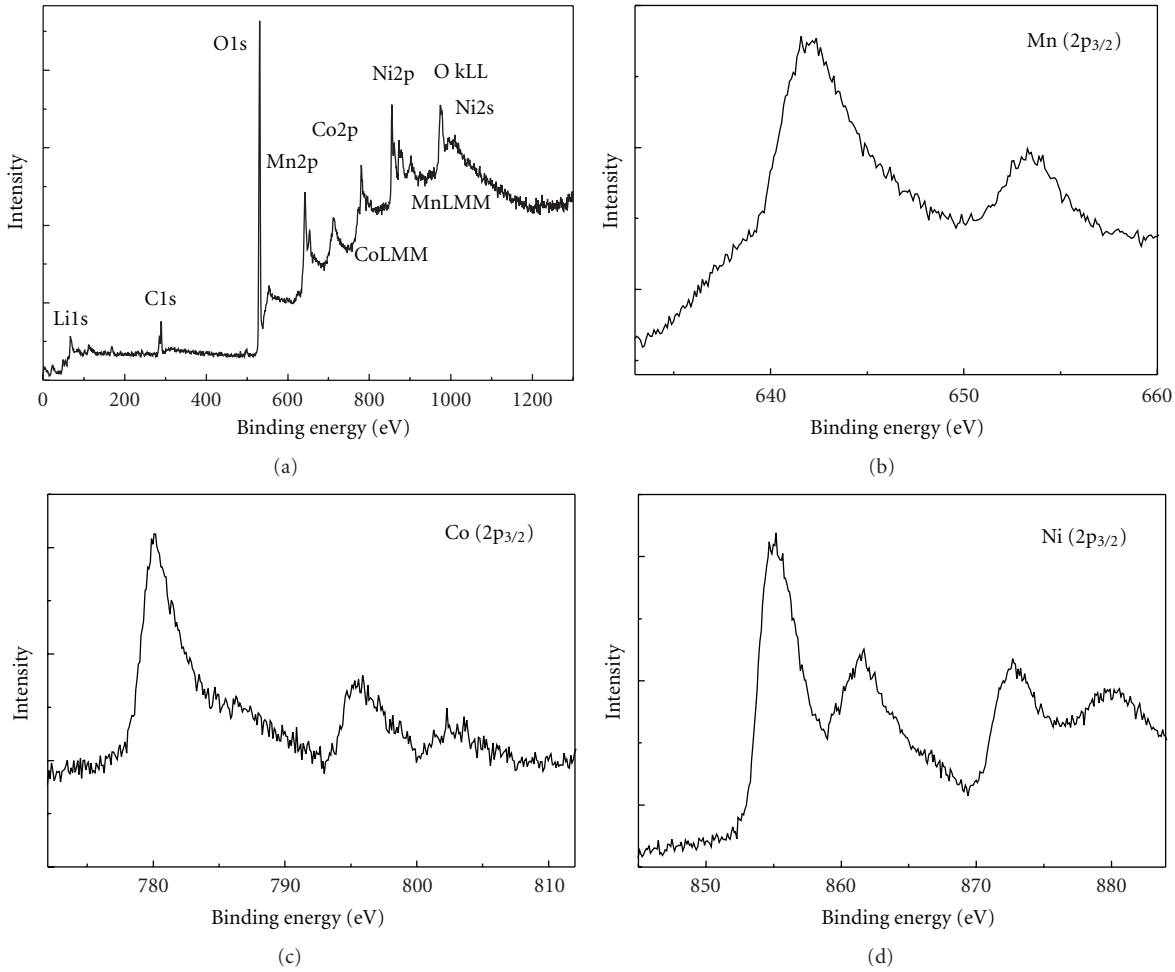

Figure 3: XPS emission spectra of (a) $Li[Ni_{0.5}Mn_{0.3}Co_{0.2}]O_2$ and magnified (b) Mn $2p_{3/2}$, (c) Co $2p_{3/2}$, and (d) Ni $2p_{3/2}$.

morphology, and it is composed of numerous primary particles with small size. The primary particle is a laminated flake minicrystal, which integrates closely into secondary particles during the precipitation process. Figure 5 shows the particle size distribution of $[Ni_{0.5}Mn_{0.3}Co_{0.2}](OH)_2$ precursor. It can be seen that there is a narrow and reasonable particle size distribution with the average grain size of 11.55 μm, which is consistent with the SEM observations. The tap density of the obtained precursor is up to 2.12 g cm^{-3}, which can be attributed to the homogeneous distributions of spherical particles with good packing properties. It is well known that the particle morphology is a very important factor on the tap density of the powder. The powder composed of spherical particles has higher tap-density than the power composed of irregular particles. The reason may be as follows. In general, there are much less agglomeration and "bridge formation" of the particles within the powder composed of spherical particles, which result in less vacancy among the particles and excellent fluidity of the powder. During tapping, the small spherical particles with excellent fluidity can easily move and occupy the vacancies among the larger particles, which leads to a small quantity of space within the powder after long period tapping [23]. Cho et al. [24] reported that the shape and size of secondary particle of the final active material could, to a great extent, depend on the morphology and size of precursor. Therefore, it is expected that the uniform-sized $[Ni_{0.5}Mn_{0.3}Co_{0.2}](OH)_2$ with spherical morphology will result in a high tap density $Li[Ni_{0.5}Mn_{0.3}Co_{0.2}]O_2$.

SEM images of the as-prepared $Li[Ni_{0.5}Mn_{0.3}Co_{0.2}]O_2$ at different magnifications are illustrated in Figure 6. It can be seen that the secondary particle of the prepared $Li[Ni_{0.5}Mn_{0.3}Co_{0.2}]O_2$ has a similar size as those of the precursor $[Ni_{0.5}Mn_{0.3}Co_{0.2}](OH)_2$ even after the precursor has been recrystallized with lithium salt during high temperature calcination. Each of the spherical particles is made up of numerous primary grains as shown in Figure 6(c). However, the shape of the primary particles for $Li[Ni_{0.5}Mn_{0.3}Co_{0.2}]O_2$ has been changed to tiny-thin plate shape with an average diameter less than 1 μm, which is much different from that for the precursor. Figure 7 shows the particle size distribution of $Li[Ni_{0.5}Mn_{0.3}Co_{0.2}]O_2$. It can be observed that the average particle size is 12.25 μm, which is a little larger than that of the precursor. This is probably attributed to addition of the lithium source and expansion of the volume during the calcination process. The tap density of the prepared $Li[Ni_{0.5}Mn_{0.3}Co_{0.2}]O_2$ is as high as 2.61 g cm^{-3}, which is

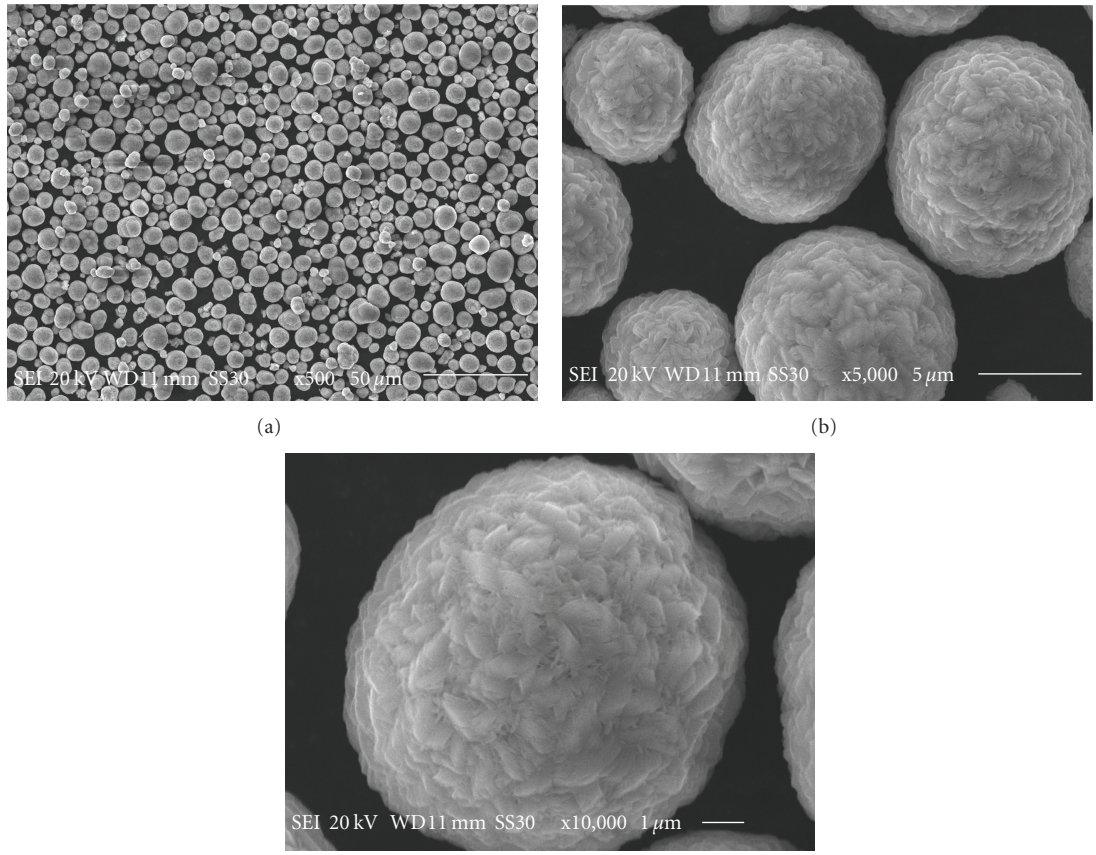

(a) (b) (c)

Figure 4: SEM of $[Ni_{0.5}Mn_{0.3}Co_{0.2}](OH)_2$ precursor at different magnifications (a) 500X, (b) 5000X, and (c) 10,000X.

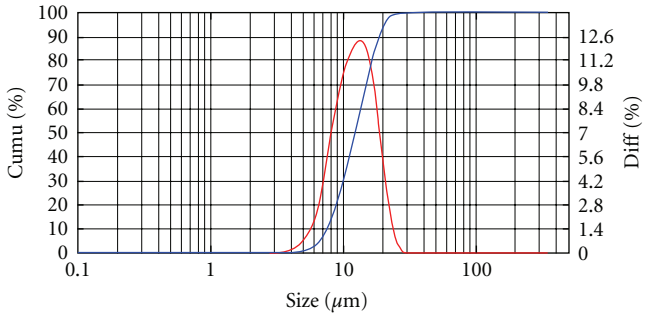

Figure 5: Particle size distribution of $[Ni_{0.5}Mn_{0.3}Co_{0.2}](OH)_2$ precursor.

close to that of commercialized $LiCoO_2$ ($2.70\,g\,cm^{-3}$) [23, 25].

The specific capacity and capacity retention of the as-prepared $Li[Ni_{0.5}Mn_{0.3}Co_{0.2}]O_2$ were measured by a coin-type cell using $Li[Ni_{0.5}Mn_{0.3}Co_{0.2}]O_2$ as active material. Initial charge and discharge profiles of $Li/Li[Ni_{0.5}Mn_{0.3}Co_{0.2}]O_2$ cell under different charge/discharge conditions are shown in Figure 8, and the corresponding cycle performance is displayed in Figure 9. Figure 8(a) shows the cell voltage plotted versus specific gravimetric capacity for the initial charge/discharge cycle operated at a current density of $32\,mA\,g^{-1}$ (0.2 C), in the voltage range of 3.0–4.3 V at 25°C. The prepared $Li[Ni_{0.5}Mn_{0.3}Co_{0.2}]O_2$ exhibits the initial discharge capacity of about $175\,mAh\,g^{-1}$ and the capacity retention is as high as 98.8% after 50 charge/discharge cycling. Even though the charge/discharge current increases to 1 C rate, the $Li[Ni_{0.5}Mn_{0.3}Co_{0.2}]O_2$ still delivers an initial discharge capacity of $166\,mAh\,g^{-1}$ (as shown in Figure 9), and the capacity retention still maintains 96.3% after 50 cycles. $Li[Ni_{0.5}Mn_{0.3}Co_{0.2}]O_2$ is only partially de-intercalated and intercalated when cells are charged and discharged in the voltage range of 3.0–4.3 V. Higher discharge capacities can be obtained when the voltage range is broadened. Figure 8(b) shows the initial charge/discharge cycle profile operated at 0.2 C between 2.5 and 4.6 V at 25°C. Initial charge and discharge capacity of 244 and $214\,mAh\,g^{-1}$ are obtained, and the capacity of $193\,mAh\,g^{-1}$ is retained at the end of 50 charge/discharge cycles with the capacity retention of 90.2%. Jouanneau et al. [26] recently reported that larger particles having higher tap-density would show less reactive at highly oxidized state in respect to thermal stability. Therefore, it is significantly critical to concern the high-temperature characteristics of the prepared $Li[Ni_{0.5}Mn_{0.3}Co_{0.2}]O_2$. Figure 8(c) presents the first charge/discharge cycle profile at 0.2 C between 3.0 and 4.3 V at 55°C. For elevated temperature test, $Li/Li[Ni_{0.5}Mn_{0.3}Co_{0.2}]O_2$ cell shows the same electrochemical behavior with the cell at room temperatures, and

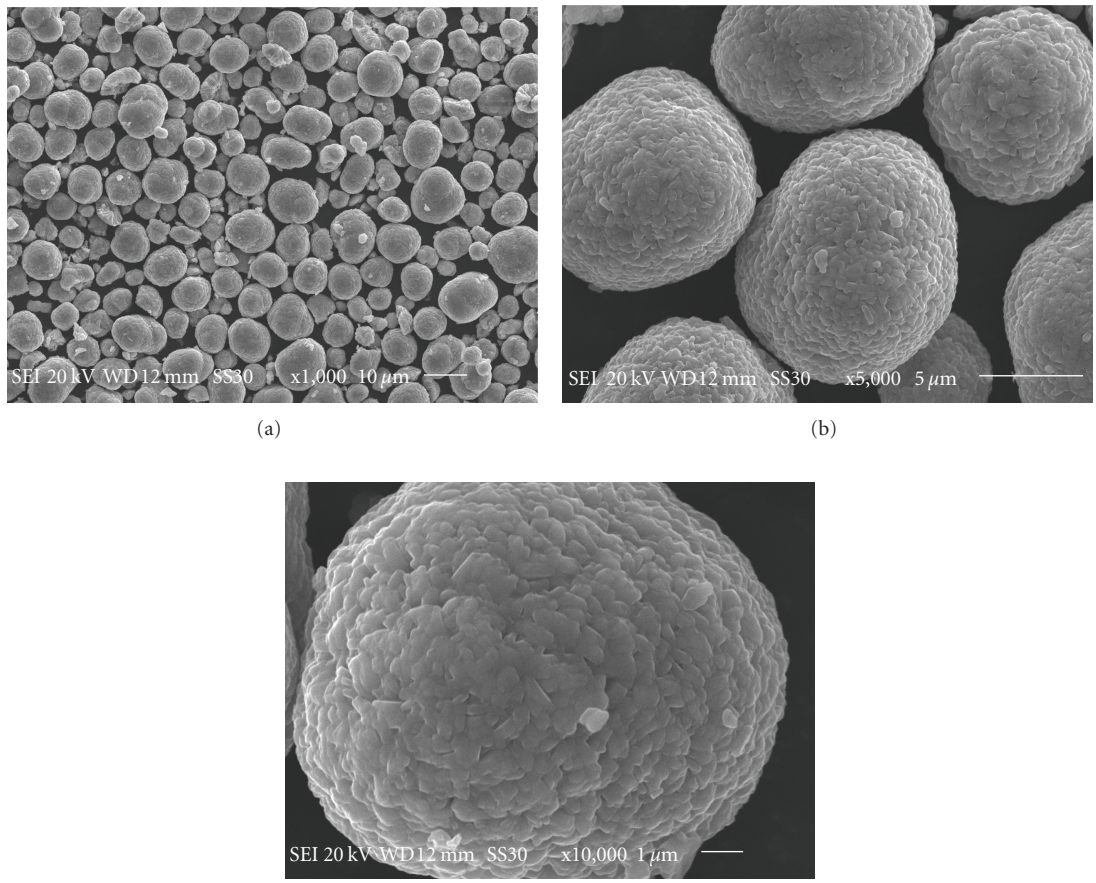

Figure 6: SEM images of the prepared $Li[Ni_{0.5}Mn_{0.3}Co_{0.2}]O_2$ at different magnifications (a) 500X, (b) 5000X, and (c) 10,000X.

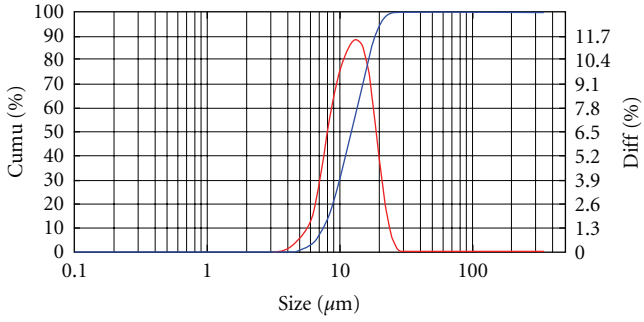

Figure 7: Particle size distribution of the prepared $Li[Ni_{0.5}Mn_{0.3}Co_{0.2}]O_2$.

it delivers higher initial discharge capacities of 180 mAh g^{-1} but with similar cycling performance as compared to room temperature; 96.7% of an initial capacity is maintained after 50 cycles (as shown in Figure 9). This notable performance of the spherical $Li[Ni_{0.5}Mn_{0.3}Co_{0.2}]O_2$ might be due to the homogeneous distribution of transition metal ions, which originates from the preparation procedure applied to the $[Ni_{0.5}Mn_{0.3}Co_{0.2}](OH)_2$ precursor in order to maintain its layered structure. That is, the mixing of the three metal salt solutions before continuous coprecipitation results in a good atomic level distribution of transition metal ions in the prepared precursor of $[Ni_{0.5}Co_{0.2}Mn_{0.3}](OH)_2$. In addition, the layered structure of $[Ni_{0.5}Mn_{0.3}Co_{0.2}](OH)_2$ allows for ready formation of a well-ordered, layered structure in $Li[Ni_{0.5}Mn_{0.3}Co_{0.2}]O_2$. The initial discharge capacity and capacity retention of the spherical $Li[Ni_{0.5}Mn_{0.3}Co_{0.2}]O_2$ prepared in the continuous co-precipitator are better than the previous results of $LiNi_{0.5}Mn_{0.5-x}Co_xO_2$ ($0 \le x \le 0.5$) materials prepared by other preparation methods [1–11, 27, 28]. Therefore, the preparation of spherical $Li[Ni_{0.5}Mn_{0.3}Co_{0.2}]O_2$ by continuous coprecipitation method could be a promising route to produce a cathode material for advanced lithium ion batteries.

It is well known that the rate capability can be affected strongly by surface texture and secondary particle size of cathode material. In order to evaluate the rate capability of the prepared $Li[Ni_{0.5}Mn_{0.3}Co_{0.2}]O_2$, the cell was charged galvanostatically with a 0.2 C (32 mA g^{-1}) rate before each discharge testing, then discharged at different C rates from 0.2 to 10 C rates stepwise. Typical discharge curves of Li/$Li[Ni_{0.5}Mn_{0.3}Co_{0.2}]O_2$ cell in the voltage range of 3.0–4.3 V and 2.5–4.6 V at various current densities are shown in

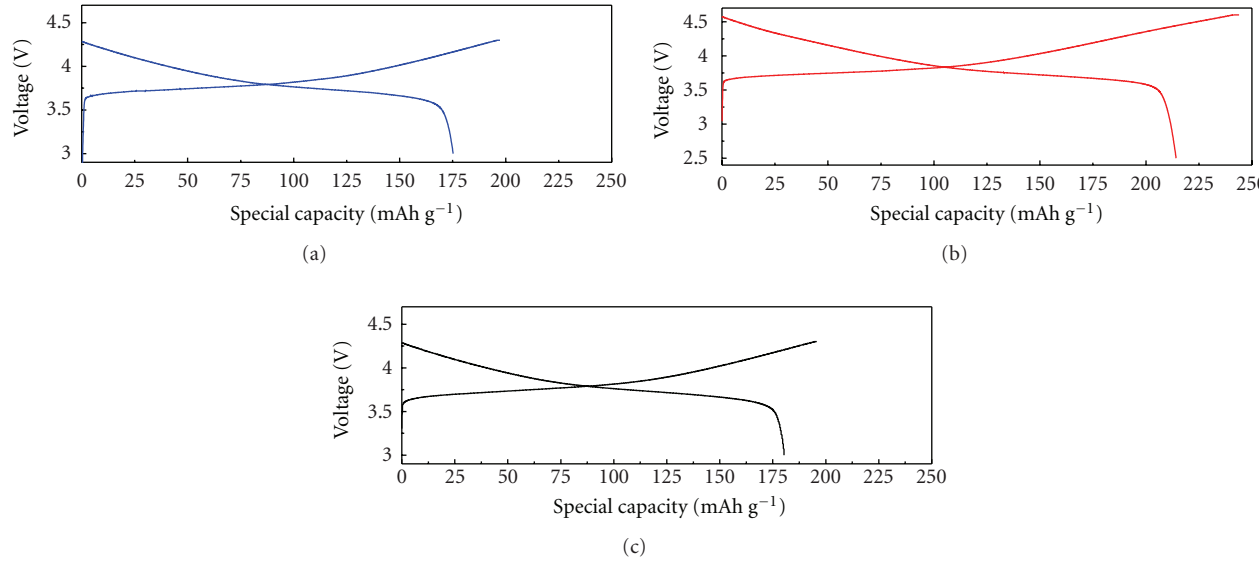

FIGURE 8: Initial charge and discharge profiles of Li/Li[$Ni_{0.5}Mn_{0.3}Co_{0.2}$]O_2 cell at a current density of 0.2 C rate under different limiting conditions: (a) 3.0–4.3 V at 25°C, (b) 2.5–4.6 V at 25°C, and (c) 3.0–4.3 V at 55°C.

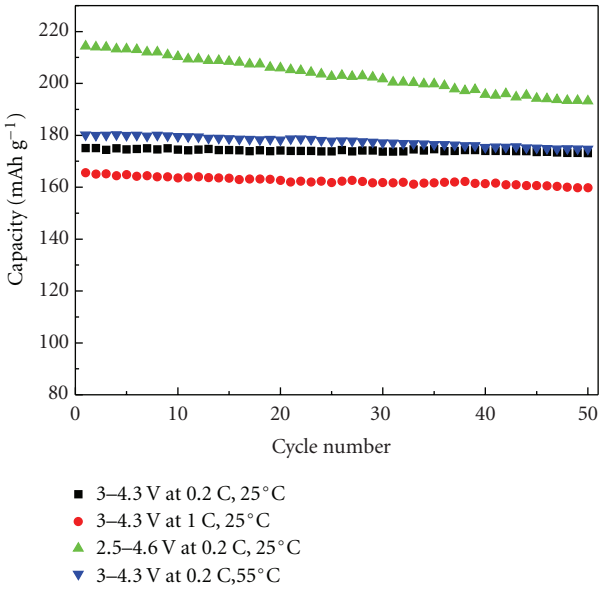

FIGURE 9: Specific discharge capacity of Li/Li[$Ni_{0.5}Mn_{0.3}Co_{0.2}$]O_2 cell as a function of cycle number under different charge/discharge conditions.

Figure 10, and their corresponding cycling performance are shown in Figure 11. From the capacity retention percentage based on 0.2 C (175 mAh g^{-1}) between 3.0 and 4.3 V as shown in Figure 10(a), the Li[$Ni_{0.5}Mn_{0.3}Co_{0.2}$]O_2 delivers a discharge capacity of 171 mAh g^{-1} at 0.5 C (the capacity retention rate is about 97.7% of that of 0.2 C), 166 mAh g^{-1} at 1 C (the capacity retention rate is about 94.5% of that of 0.2 C), 153 mAh g^{-1} at 2 C (the capacity retention rate is about 88% of that of 0.2 C), and 135 mAh g^{-1} at 5 C (the capacity retention rate is about 78.5% of that of 0.2 C). Even at 10 C (1600 mA g^{-1}), the capacity of Li[$Ni_{0.5}Mn_{0.3}Co_{0.2}$]O_2 is still as high as 116 mAh g^{-1} and the capacity retention rate is about 66.1% of that of 0.2 C. While the voltage range is broadened up to 2.5–4.6 V (as shown in Figure 10(b)), the Li[$Ni_{0.5}Mn_{0.3}Co_{0.2}$]O_2 still retains a high percentage of its discharge capacity at high currents during cycling process, the capacity retention percentage at 0.5 C, 1 C, 2 C, 5 C, and 10 C based on 0.2 C capacity (214 mAh g^{-1}) are 95.7%, 92.5%, 85.4%, 74.5%, and 63.1%, respectively. The enhanced discharge capacity at accelerated rates clearly demonstrates the advantages of the spherical secondary particles. Compared with the irregular particles reported in literatures [3, 6, 9], the spherical particles with close-packed primary grains in this work will likely improve interparticle lithium ion movement, thereby enhancing the rate capability of the material.

4. Conclusions

Li[$Ni_{0.5}Mn_{0.3}Co_{0.2}$]O_2 prepared by the continuous hydroxide coprecipitation shows a homogeneous spherical morphology with well-ordered layered structure and has high tap density of 2.61 g cm^{-3}, which is close to that of commercialized $LiCoO_2$. The Li[$Ni_{0.5}Mn_{0.3}Co_{0.2}$]O_2 displays high initial discharge capacity of 175 mAh g^{-1} (3–4.3 V, 0.2 C, 25°C), 166 mAh g^{-1} (3–4.3 V, 1 C, 25°C), and 214 mAh g^{-1} (2.5–4.6 V, 0.2 C, 25°C), as well as good cycling performance. In addition, it exhibits good high-temperature characteristics and excellent rate capability. The good electrochemical performance of Li[$Ni_{0.5}Mn_{0.3}Co_{0.2}$]O_2 can be attributed to its structure integrity and the existence of mixed-valance cations (Ni^{2+}/Ni^{3+}). Therefore, it is concluded that the spherical Li[$Ni_{0.5}Mn_{0.3}Co_{0.2}$]O_2 powder prepared by the continuous coprecipitation method is a promising cathode material for advanced lithium ion batteries.

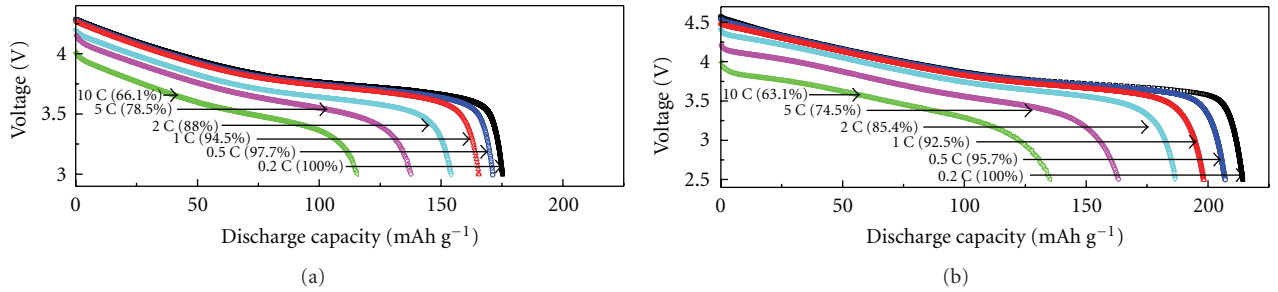

FIGURE 10: Typical discharge curves of Li/Li[$Ni_{0.5}Mn_{0.3}Co_{0.2}$]O_2 cell in the voltage range of (a) 3.0–4.3 V and (b) 2.5–4.6 V at various current densities at 25°C.

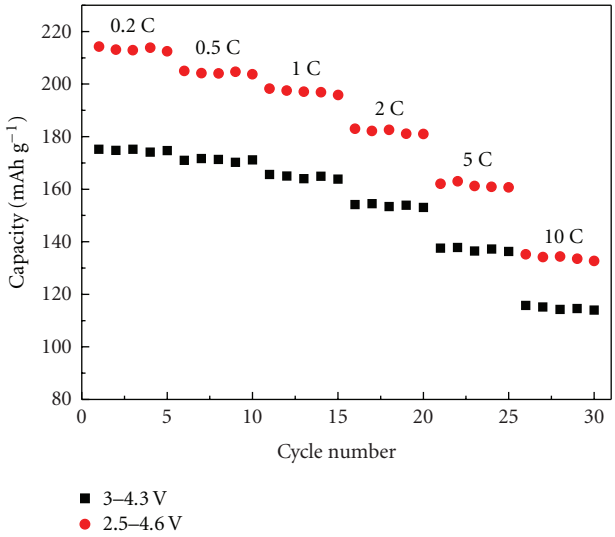

FIGURE 11: Cycle performance of Li/Li[$Ni_{0.5}Mn_{0.3}Co_{0.2}$]O_2 cell in the voltage range of 3.0–4.3 V and 2.5–4.6 V at various current densities at 25°C.

Acknowledgments

This paper was financially supported by the National Natural Science Foundation of China under project no. 20871101, scientific and technological plan project of Ministry of Science and Technology no. 2009GJD20021, Joint Fund of Natural Science of Hunan Province and Xiangtan City under project no. 09BG005, Industrial Project of Colleges and Universities of Hunan Province under project no. 10CY005, Project of Condition Research of Hunan Province under project no. 2010TC2004, and Colleges and Universities in Hunan Province plans to graduate research and innovation under project no. CX2009B133.

References

[1] Z. Lu, L. Y. Beaulieu, R. A. Donaberger, C. L. Thomas, and J. R. Dahn, "Synthesis structure, and electrochemical behavior of Li[$Ni_xLi_{(1-2x)/3}Mn_{(2-2x)/3}$]$O_2$," *Journal of the Electrochemical Society*, vol. 149, no. 6, pp. A778–A791, 2002.

[2] T. Ohzuku and Y. Makimura, "Layered lithium insertion material of $LiNi_{1/2}Mn_{1/2}O_2$: a possible alternative to $LiCoO_2$ for advanced lithium-ion batteries," *Chemistry Letters*, no. 8, pp. 744–745, 2001.

[3] Y. Makimura and T. Ohzuku, "Lithium insertion material of $LiNi_{1/2}Mn_{1/2}O_2$ for advanced lithium-ion batteries," *Journal of Power Sources*, vol. 119-121, pp. 156–160, 2003.

[4] Z. Lu, D. D. MacNeil, and J. R. Dahn, "Layered cathode materials Li[$Ni_xLi_{(1/3-2x/3)}Mn_{(2/3-x/3)}$]$O_2$ for lithium-ion batteries," *Electrochemical and Solid-State Letters*, vol. 4, no. 11, pp. A191–A194, 2001.

[5] M. E. Spahr, P. Novák, O. Haas, and R. Nesper, "Cycling performance of novel lithium insertion electrode materials based on the Li-Ni-Mn-O system," *Journal of Power Sources*, vol. 68, no. 2, pp. 629–633, 1997.

[6] D. C. Li, T. Muta, and H. Noguchi, "Electrochemical characteristics of $LiNi_{0.5}Mn_{0.5-x}Ti_xO_2$ prepared by solid state method," *Journal of Power Sources*, vol. 135, no. 1-2, pp. 262–266, 2004.

[7] S. Jouanneau, D. D. MacNeil, Z. Lu, S. D. Beattie, G. Murphy, and J. R. Dahn, "Morphology and Safety of Li[$Ni_xCo_{1-2x}Mn_x$]O_2 ($0 \le x \le 1/2$)," *Journal of the Electrochemical Society*, vol. 150, no. 10, pp. A1299–A1304, 2003.

[8] B. L. Cushing and J. B. Goodenough, "Influence of carbon coating on the performance of a $LiMn_{0.5}Ni_{0.5}O_2$ cathode," *Solid State Sciences*, vol. 4, no. 11-12, pp. 1487–1493, 2002.

[9] D. C. Li, Y. Sasaki, K. Kobayakawa, and Y. Sato, "Impact of cobalt substitution for manganese on the structural and electrochemical properties of $LiMn_{0.5}Ni_{0.5}O_2$," *Electrochimica Acta*, vol. 51, no. 18, pp. 3809–3813, 2006.

[10] Z. L. Liu, A. S. Yu, and J. Y. Lee, "Synthesis and characterization of $LiNi_{1-x-y}Co_xMn_yO_2$ as the cathode materials of secondary lithium batteries," *Journal of Power Sources*, vol. 81-82, pp. 416–419, 1999.

[11] D. C. Li, Y. Sasaki, M. Kageyama, K. Kobayakawa, and Y. Sato, "Structure, morphology and electrochemical properties of $LiNi_{0.5}Mn_{0.5-x}Co_xO_2$ prepared by solid state reaction," *Journal of Power Sources*, vol. 148, no. 1-2, pp. 85–89, 2005.

[12] Joint Committee on Powder Diffraction Standards, card no. 03–0177.

[13] K. S. Park, M. H. Cho, S. J. Jin, and K. S. Nahm, "Structural and electrochemical properties of nanosize layered Li[$Li_{1/5}Ni_{1/10}Co_{1/5}Mn_{1/2}$]$O_2$," *Electrochemical and Solid-State Letters*, vol. 7, no. 8, pp. A239–A241, 2004.

[14] A. Rougier, P. Gravereau, and C. Delmas, "Optimization of the composition of the $Li_{1-z}Ni_{1+z}O_2$ electrode materials: structural, magnetic, and electrochemical studies," *Journal of the Electrochemical Society*, vol. 143, no. 4, pp. 1168–1175, 1996.

[15] T. Ohzuku, A. Ueda, and M. Nagayama, "Electrochemistry and structural chemistry of $LiNiO_2$ ($R\bar{3}m$) for 4 volt secondary

lithium cells," *Journal of the Electrochemical Society*, vol. 140, no. 7, pp. 1862–1870, 1993.

[16] W. Li, J. N. Reimers, and J. R. Dahn, "In situ x-ray diffraction and electrochemical studies of $Li_{1-x}NiO_2$," *Solid State Ionics*, vol. 67, no. 1-2, pp. 123–130, 1993.

[17] P. Y. Liao, J. G. Duh, and S. R. Sheen, "Effect of Mn content on the microstructure and electrochemical performance of $LiNi_{0.75-x}Co_{0.25}Mn_xO_2$ cathode materials," *Journal of the Electrochemical Society*, vol. 152, no. 9, pp. A1695–A1700, 2005.

[18] J. N. Reimers, E. Rossen, C. D. Jones, and J. R. Dahn, "Structure and electrochemistry of $Li_xFe_yNi_{1-y}O_2$," *Solid State Ionics*, vol. 61, no. 4, pp. 335–344, 1993.

[19] K. M. Shaju, G. V. Subba Rao, and B. V. R. Chowdari, "Performance of layered $Li(Ni_{1/3}Co_{1/3}Mn_{1/3})O_2$ as cathode for Li-ion batteries," *Electrochimica Acta*, vol. 48, no. 2, pp. 145–151, 2002.

[20] S. Madhavi, G. V. Subba Rao, B. V. R. Chowdari, and S. F. Y. Li, "Synthesis and cathodic properties of $LiCo_{1-y}Rh_yO_2(0 \leq y \leq 0.2)$ and $LiRhO_2$," *Journal of the Electrochemical Society*, vol. 148, no. 11, pp. A1279–A1286, 2001.

[21] Y. Sun, C. Ouyang, Z. Wang, X. Huang, and L. Chen, "Effect of Co content on rate performance of $LiMn_{0.5-x}Co_{2x}Ni_{0.5-x}O_2$ cathode materials for lithium-ion batteries," *Journal of the Electrochemical Society*, vol. 151, no. 4, pp. A504–A508, 2004.

[22] M. Thackeray, "Lithium-ion battries: an unexpected conductor," *Nature Materials*, vol. 1, no. 2, pp. 81–82, 2002.

[23] J. R. Ying, C. Y. Jiang, and C. R. Wan, "Preparation and characterization of high-density spherical $LiCoOM_2$ cathode material for lithium ion batteries," *Journal of Power Sources*, vol. 129, no. 2, pp. 264–269, 2004.

[24] T. H. Cho, S. M. Park, M. Yoshio, T. Hirai, and Y. Hideshima, "Effect of synthesis condition on the structural and electrochemical properties of $Li[Ni_{1/3}Mn_{1/3}Co_{1/3}]O_2$ prepared by carbonate co-precipitation method," *Journal of Power Sources*, vol. 142, no. 1-2, pp. 306–312, 2005.

[25] P. He, H. Wang, L. Qi, and T. Osaka, "Synthetic optimization of spherical $LiCoO_2$ and precursor via uniform-phase precipitation," *Journal of Power Sources*, vol. 158, no. 1, pp. 529–534, 2006.

[26] S. Jouanneau, K. W. Eberman, L. J. Krause, and J. R. Dahn, "Synthesis, characterization, and electrochemical behavior of improved $Li[Ni_xCo_{1-2x}Mn_x]O_2$ $(0 \leq x \leq 1/2)$," *Journal of the Electrochemical Society*, vol. 150, no. 12, pp. A1637–A1642, 2003.

[27] S. B. Kim, K. J. Lee, W. J. Choi et al., "Preparation and cycle performance at high temperature for $Li[Ni_{0.5}Co_{0.2}Mn_{0.3}]O_2$ coated with $LiFePO_4$," *Journal of Solid State Electrochemistry*, vol. 14, no. 6, pp. 919–922, 2010.

[28] L. Xiao, X. Liu, X. Zhao, H. Liang, and H. Liu, "Preparation of $LiNi_{0.5}Mn_{0.5}O_2$ cathode materials by urea hydrolysis coprecipitation," *Solid State Ionics*, vol. 192, pp. 335–338, 2011.